ENG Transactions

Journal homepage: http://www.engtransactions.com

ENG Transactions, vol. 3, pp. 1-11, March 2022
ID: ENGT-2203052112744

Research Article

Magnetic Nanofluid Temperature Distribution with Different Concentrations and Diffusion of MNPs

Mohammad Mohammadzadeh[1*], Erfan Rahmanian[2], Shima Tabakhi[3], Amin Mohammadzadeh[4]

[1,3] *School of Electrical, Computer, and Biomedical Engineering, Southern Illinois University Carbondale, IL, USA*
[2] *Department of Biomechanical Engineering, Iran University of Science and Technology, Tehran, Iran*
[4] *Department of Civil and Environmental Engineering, University of Louisville, Louisville, KY, USA*

Keywords

Magnetic fluid hyperthermia,
Nanofluid,
Nanoparticles distribution,
Specific absorption rate.

Abstract

Hyperthermia therapy using magnetic nanofluid is one method to regulate and optimize temperature, which is a substantial challenge in practice. The generated heat through the magnetic coil using magnetic nanoparticles in the tumor is closely associated with the dispersion of particles, frequency, magnetic field intensity, and the property of the tissue. Therefore, with magnetic nanoparticles injected into tumor tissue and subjects to an alternating magnetic field with high amplitude and frequency, tumor tissue temperature rises, which could lead to destroying cancer cells. In this study, to simulate the magnetic field intensity at different parts of the experiment and to solve heat transfer equation, a finite element method using COMSOL Multiphysics has been used. Then, to verify our model, an experimental setup was used to measure temperature distribution in an agarose gel with two different nanofluid concentrations for dispersed and concentrated injections. Simulation results have been compared with experimental ones to show the model's accuracy. Results indicate that the magnetic field in different parts of the gel is not the same, but the differences are insignificant. Temperature distribution for both types of nanofluid in dispersed and concentrated injections has a behavior like a polynomial function with a degree of three. Compared to dispersed injection, a higher temperature is observed in concentrated injection.

1. Introduction

The nanomagnetic fluid is injected into the target tissue under a high frequency and intensity field in hyperthermia treatment. This field rotates the particles and generates heat inside the tissue, consequently. The generated heat will destroy the cancer cells. It's not always possible to do the experiment mentioned above on living tissue, and the reason is that we need to protect the living part of the tissue. Therefore, to conduct our experiments, we must choose an environment with the same characteristics as living tissue. Hyperthermia uses physical methods to heat determined tissues to temperatures in the range of 40–46 °C with a treatment

* **Corresponding Author:** Mohammad Mohammadzadeh
E-mail address: mohammad.mohammadzadeh@siu.edu

Academic Editor: Hafiz Mudassir Munir

Received: 31 January 2022; **Revised:** 22 February 2022; **Accepted:** 5 March 2022
https://doi.org/10.52547/engt.3.2203052112744

Citation: M. Mohammadzadeh, E. Rahmanian, S. Tabakhi, A. Mohammadzadeh "Magnetic nanofluid temperature distribution with different concentrations and diffusion of MNPs," *ENG Transactions*, vol. 3, pp. 1-11, 2022.

time of approximately one hour [1-3]. Research has shown that high temperatures can damage and kill cancer cells, usually with minimal injury to normal tissues. It is proposed that hyperthermia may shrink tumors by killing cancer cells and injuring proteins and structures within the cells to make the cells more sensitive to radiation therapy (RT) and chemotherapy [4]. In some cases, if the elevated temperature is utilized as the stand-alone technique, tissue temperature above 48 degrees would be the objective. However, magnetic fluid hyperthermia is not widely applicable in clinical treatments due to the difficulty in accurately determining temperature distribution within the target tissue, precise control of thermal dose, and uniform heating [5]. Most investigations and clinical applications have focused on the effects of heating and specific absorption rates (SAR) of magnetic fluids [5].

The precise temperature measuring in tissue boundaries and evaluating nanoparticles distribution in tissue are other problems for experimenting on living tissue. To do so, we chose agarose gel because it has been proven that a gel has a porous environment like living tissue, and it is an appropriate environment for experimenting with drug delivery problems. The gel is used for drug delivery studies in some research. As a matter of fact, gel is a mid-environment between liquid and solid combined with solid matrices and water cavities. Various densities of gel represent different tissues. Lee et al.[6] studied the hyperthermia process in two ways: solving or injecting nanoparticles in the gel. The temperature distribution and generated microscopic structure have been studied for each method. Rahn et al. [7] used a cylindrical two layers gel that inner and outer cylinders represent tumor and healthy tissues, respectively. The Pennes bio-heat transfer equation model has been used many times in different bio-heat models [8]. This model shows the effect of blood perfusion as a temperature-dependent heat sink term and practically simulates convection heat transfer of blood. The blood perfusion effect is assumed to be homogeneous and isotropic, and thermal equilibration occurs in the micro-circulatory capillary bed. Due to tissues' complications and complex geometry, exact solutions are unavailable in many cases [9]. In many practical applications, numerical models such as the finite element method [10-15], finite difference method [16-19], Monte Carlo method [20, 21],and lattice Boltzmann method are used [22], in which homogenous nanoparticles distribution or heat generation inside tumor and healthy tissue have been considered. Furthermore, permanent magnet manipulators are employed to control a particle movement inside a container filled by fluid to explore noninvasive drug targeting procedures. These systems utilizing permanent magnet to manipulate magnetic objects from a distance without direct connection by generating magnetic field and correctly controlling the shape of this field [13-15].

In this paper, experimental and simulation results obtained from agarose gel in a cylindrical environment are compared for uniform and concentrated distributions. Influence of the collective behaviors of nanoparticles in suspension are significant [23]. The results show how significant is the relationship between temperature distribution with respect to the density and distribution of the nanoparticles. It is worth mentioning that in hyperthermia treatment with magnetic nanoparticles, the temperature distribution is one of the most critical factors. By comparing experimental data with calculated temperature regarding to heat generation inside an agar gel, the numerical procedure is validated. Since nanoparticle distribution in tumors is a primary factor determining the resulting heating pattern and therapeutic outcome of magnetic hyperthermia treatment, by using determined nanoparticles distribution proposed by Salloum et al. [24] and power dissipation equation, we calculated heat generation source in heat transfer equation and abled to find temperature variation inside Agarose gel. The main advantage of this work is using real particles distribution and finding heat generation inside the gel according to several parameters like a magnetic field, frequency, and amplitude.

2. Experiment Necessity

The intensity of the periodic external field should be measured precisely. The magnetic coil produced by “Cancer Models Research Center (CMRC)” located at Iran University of Science and Technology is used for this study, as shown in Figure 1.

Figure 1. The designed coil as the setup for the experiments

This coil consists of ten loops. These loops are made of copper pipes with inner and outer radii of 1mm and 2.5 mm, respectively. The inner radius of the coil is 35 mm. The nanofluid used in this experiment contains a suspension of Fe_3O_4 nanoparticles in water with a density of 7%. Since the greater value of the density will increase the temperature more than the average body temperature and could destroy healthy tissue, this nanoparticle with this specific value of density is fit for this experiment. The characteristic of the nanoparticles is summarized in Table 1[10].

Table 1. Characteristic of Fe_3O_4

Parameters	Nano Particle Diameter (nn)	Density (kg/m^3)	Specific Heat (J/kg.K)	Heat Transfer Coef. (w/m.K)	Saturation Magnetization (Guss)
Symbol	d	ρ	C	k	M_z
Value	8	4950	670	60	300

The gel is produced by solving uniformly $1gr$ agarose powder in $100cc$ boiling water. Gel density is $1000Kg/m^3$, its heat transfer coefficient is $0.566w/mk$, and its specific heat is $3900\,j/Kg.k$ [12]. The samples characteristics should be calculated separately by the following equations, especially in the stage that nanoparticles distribute uniformly in the gel. φ is the volume fraction of nanoparticles. Also, density and specific heat for the section that nanoparticles and gel are mixed will be obtained by Eq. (1), (2), and (3) and their values are shown in Table 2.

$$\varphi = \frac{V_{nano\ particles}}{V_{mixture}} \tag{1}$$

$$\rho_{mixture} = \varphi\rho_{nano\ particles} + (1-\varphi)\rho_{gel} \tag{2}$$

$$C_{mixture} = \varphi C_{nano\ particles} + (1-\varphi)C_{gel} \tag{3}$$

Table 2. Characteristic of the mixture of nonofluid and gel

Mixture property	Symbol	Value
Mixture Heat Capacity	c_{mix}	3890.31 ($Jkg^{-1}K^{-1}$)
Heat Conductivity	k_{mix}	0.566 ($Wm^{-1}k^{-1}$)
Density	ρ_{mix}	1011.85(kgm^{-3})

3. Uniform Distribution of Nano Particles in Cylindrical Gel

Two different values of $0.2cc$ and $0.1cc$ of nano particles with capacity of 0.7 are injected in cylindrical gel with volume of $15cc$, uniformly and are placed in field separately. The cylinder radius and its height are $30mm$ and $5mm$, respectively. Two experimental samples are shown in Figure 2.

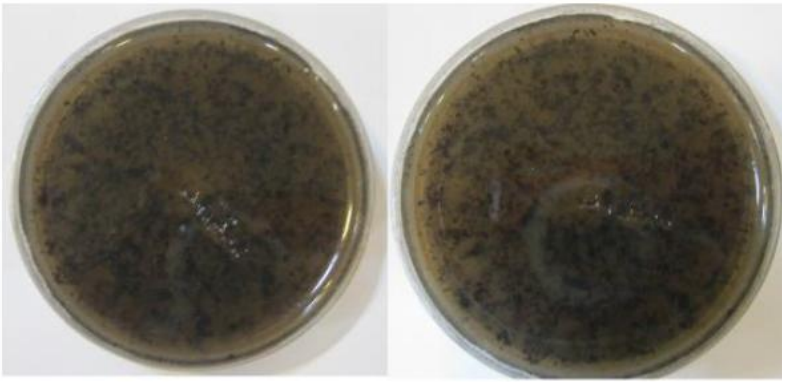

Figure 2. Left, 0.2cc ; right 0.1cc uniform injection.

Also, we implemented a finite element method using COMSOL software for this work. The coupled equations of field and heat are as blow.

$$jw\,\sigma(\mathrm{T})\,\mathrm{A}+\nabla\times(\mu^{-1}\nabla\times A)=0 \tag{4}$$

$$\rho c_P\frac{\partial T}{\partial t}-\nabla k\,\nabla T=Q(\mathrm{T},\mathrm{A}) \tag{5}$$

In Eq. 5 $Q(\mathrm{T},\mathrm{A})$ is induced heat by the magnetic field. The electrical resistance of the coil is 4×10^{-6}, the frequency is 50 Hz, the electrical potential is $184v$ and $146A$. In this simulation, irregular and triangular meshing is used. As shown in Figure 3, the field variation range by averaging is $7.2KA/m$. This value is constant for both injections because the dose of nanoparticles does not affect the field.

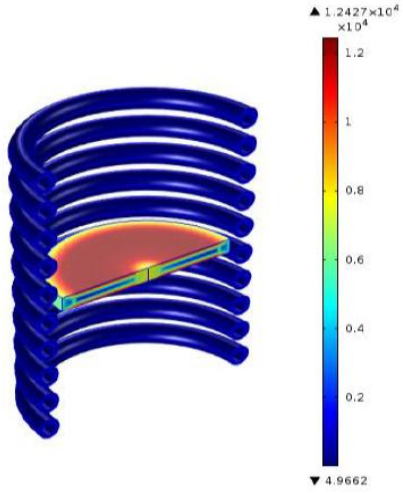

Figure 3. Magnetic field intensity (dispersed distribution)

The COMSOL software uses the following equation to calculate the temperature distribution.

$$\rho_{mixture}C_{mixture}\frac{\partial T}{\partial t}=\nabla.(\mathrm{k}_{mixture}.\nabla T)+\mathrm{Q}_g \tag{6}$$

where Q_g is the energy that is generated by nanoparticles in tissue and obtained by Eq. (7) [13].

$$P=\pi\mu_0 x_0 H_0^2 f\,\frac{2\pi f\,\tau}{1+(2\pi f\,\tau)^2} \tag{7}$$

where μ_0 is vacuum permeability and $\mu_0=4\pi\times10^{-7}Tm/A$, x_0 is equivalent sensitivity, H_0 is field intensity, f is field frequency and τ is effective rest time that is:

$$\tau_N=\frac{\sqrt{\pi}}{2}\tau_0\frac{\exp(\Gamma)}{\sqrt{\Gamma}} \tag{9}$$

$$\tau_B = \frac{3\eta V_H}{kT} \tag{10}$$

From Eq. (9) and Eq. (10), the shortest time is the dominant parameter in the adequate time. τ_0 is mean rest time, η is fluid viscosity, V_H is the hydrodynamic volume of nanoparticles, k is Boltzmann constant ($1.38\times10^{-23} JK^{-1}$), and T is the absolute temperature. The Γ is another parameter defined by:

$$\tau_B = \frac{KV_M}{kT} \tag{11}$$

In Eq. 11, K is a constant related to the material of nanoparticles, V_M is nanoparticle's volume and, V_h is nanoparticle's volume with coverage thickness (Hydrodynamic volume).

$$V_H = \frac{\pi(\mathrm{D}+2\delta)^3}{6} \tag{12}$$

$$V_M = \frac{\pi V_M}{6} \tag{13}$$

In Eq. (12) and Eq. (13), D is nanoparticle's diameter and δ is coverage thickness. The equivalent sensitivity, by $M/M_s = \coth\xi - 1/\xi$, is defined as below:

$$x_0 = x_i \frac{3}{\xi}(\coth\xi - \frac{1}{\xi}) \tag{14}$$

In Eq. 14, $H = H_0\cos(\omega \mathrm{t})$, $\xi = \mu_0 M_d H V_M / kT$, $M_s = \phi M_d$, $\omega = 2\pi f$ and ϕ is volume fraction of the nanoparticles. M_d and M_s are magnetization range and saturation, respectively. Initial sensitivity defines as:

$$x_i = \frac{\mu_0 \phi M_d^2 V_M}{3kT} \tag{15}$$

P is 0.065×10^5 and $0.033\times10^5 w/m^3$ for .2cc and .1cc injections, respectively. The initial temperature of the sample is $20\,^{\circ}C$, and the heat convection coefficient is 10. The temperature distribution in the gel after applying an $1800s$ magnetic field for $0.2cc$ and $0.1cc$ injections is shown in Figure 4.

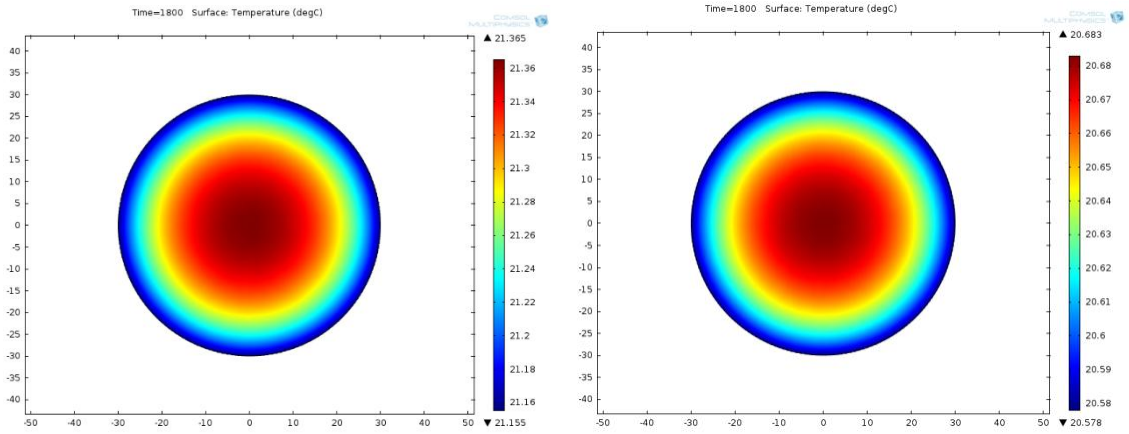

Figure 4. Left, $0.2cc$; right $0.1cc$ temperature distribution for uniform injection at $1800s$.

4. Comparison of Experimental and Simulation Results in Uniform Distribution

The central point of the cylinder for both samples ($0.1cc$ and $0.2cc$) is measured every $120s$ up to $1800s$. The results are compared with simulation ones in Figure 5.

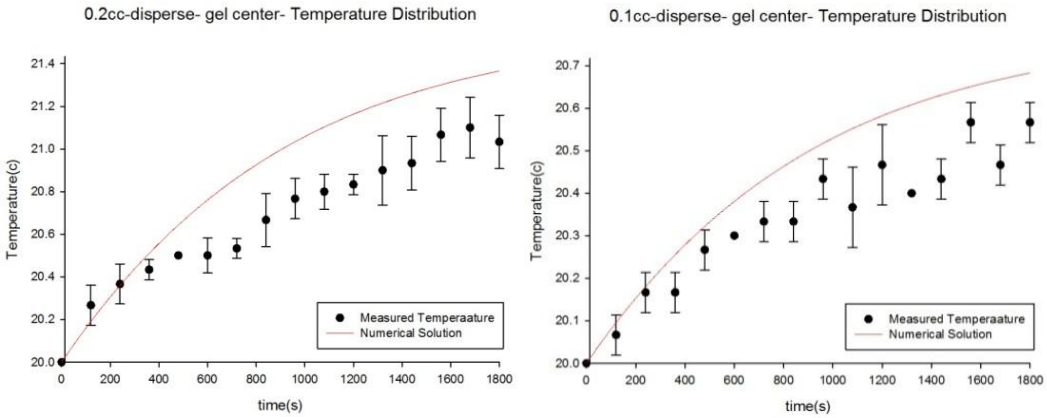

Figure 5. Left, 0.2*cc* ; right 0.1*cc* temperature variation with respect to the time for uniform injection in center point.

The results those have been obtained for different temperature along cylinder radius, are illustrated in Figure 6.

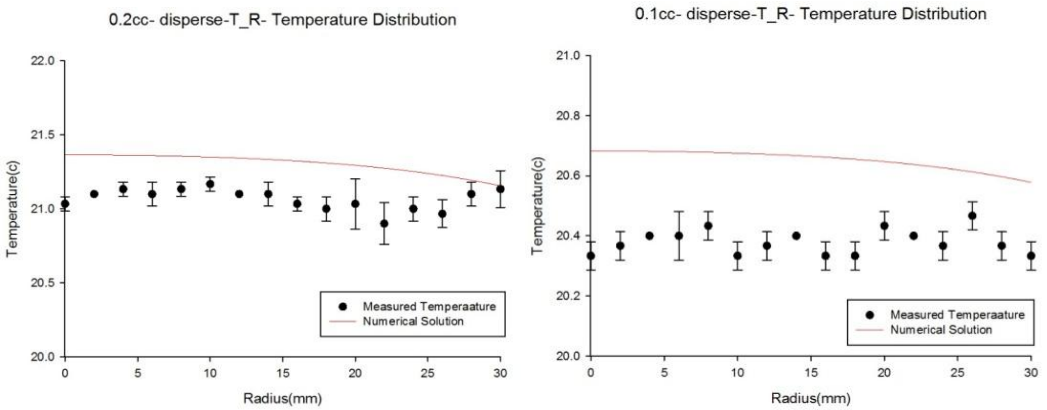

Figure 6. Left, 0.2*cc* ; right 0.1*cc* temperature variation with respect to the radius for uniform injection.

It is obvious that in uniform injection, temperature change along radius is negligible. The results show an appropriate correlation between experiment and simulation.

5. Concentrated Distribution of Nano Particles in Gel

In concentrated distribution, nano particles are only injected in a section of gel and the temperature distribution will not uniform, accordingly. In Figure 7, two experimental samples are shown. The height of cylinder section that includes nano particles and gel is $5mm$ and radii for $0.1cc$ and $0.2cc$ injections, are $11mm$ and $8.5mm$, respectively. The total volume of gel is $15cc$, its height is $5mm$ and its radius is $30mm$.

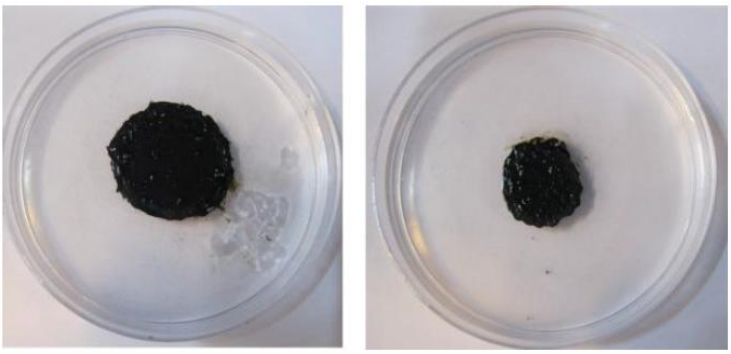

Figure 7. Left, 0.2*cc* ; right 0.1*cc* concentrated injection in agarose gel.

In simulation, the voltage is $184v$, current is $146A$ and frequency is $50Hz$. In Figure 8, the simulation results for .2cc concentrated injection is shown.

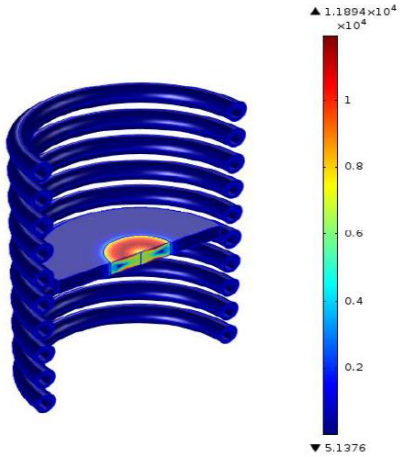

Figure 8. Magnetic field intensity (concentrated distribution)

This figure shows that there is not significant different between field distribution in uniform and concentrated one and so the nano particle density does not have effect on field. Therefore, field intensity is same as before ($7.2KA/m$).

The generated heat in $0.1cc$ and $0.2cc$ injections, are $70742.47w/m^2$ and $48655.2w/m^2$, respectively. In Figure 9, the temperature distributions in gel after $1800s$, is shown. It could be concluded that in concentrated distribution temperature increment is more than uniform distribution, obviously. Also, in $0.2cc$ injection temperature increased more than $0.1cc$ injection.

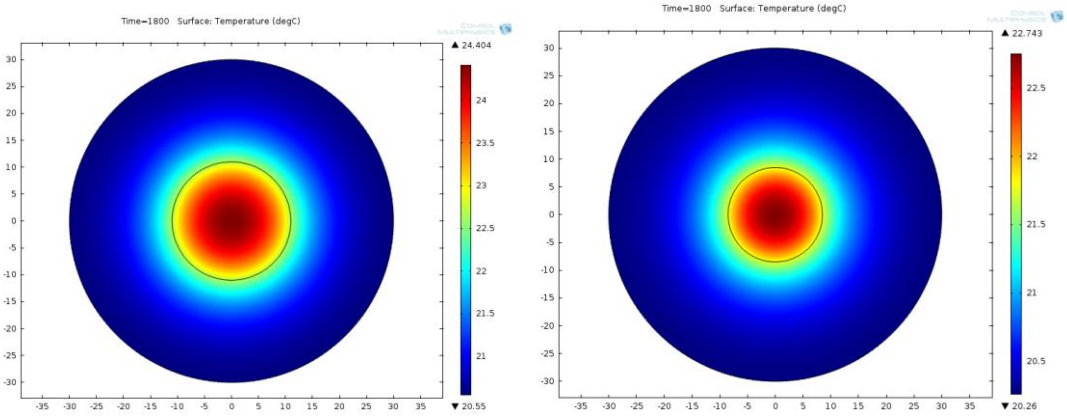

Figure 9. Left, $0.2cc$; right $0.1cc$ temperature distribution for concentrated injection at $1800s$.

6. Experimental and Simulation Results Comparison in Concentrated Distribution

The central temperature of cylinder for both .2cc and .1cc injections, is measured every $120s$ up to $1800s$ and compared with simulation one in Figure 10.

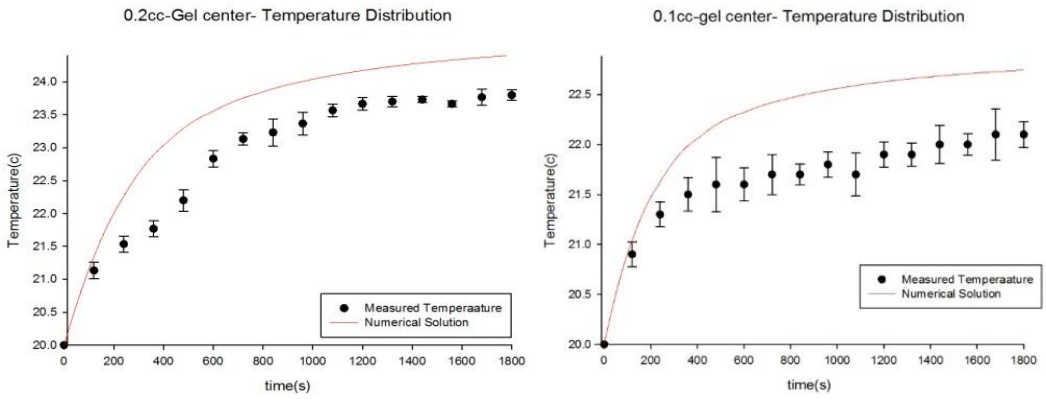

Figure 10. Left, $0.2cc$; right $0.1cc$ temperature variation with respect to the time for concentrated injection in center point.

In Figures 11, the temperature variation along cylinder radius is illustrated.

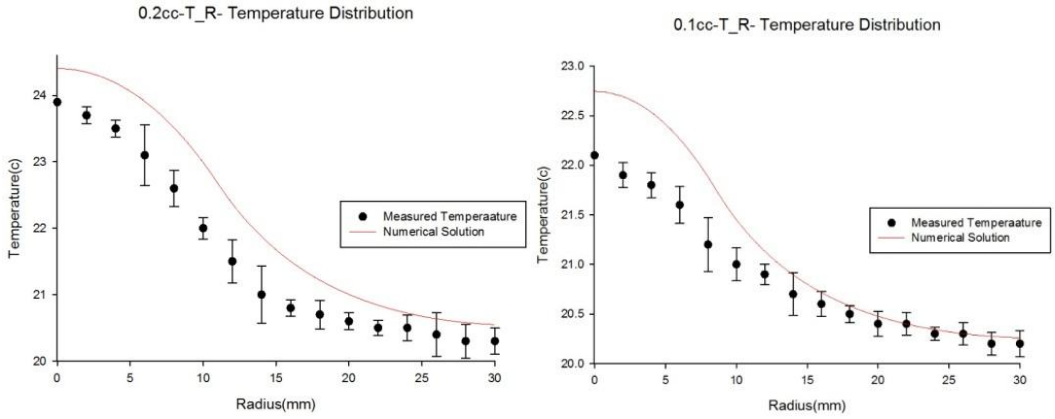

Figure 11. Left, 0.2*cc* ; right 0.1*cc* temperature variation with respect to the radius for concentrated injection.

This section shows that the difference between simulation and experiment results is not significant. Even after almost 25 seconds, we can see how close these results are to each other.

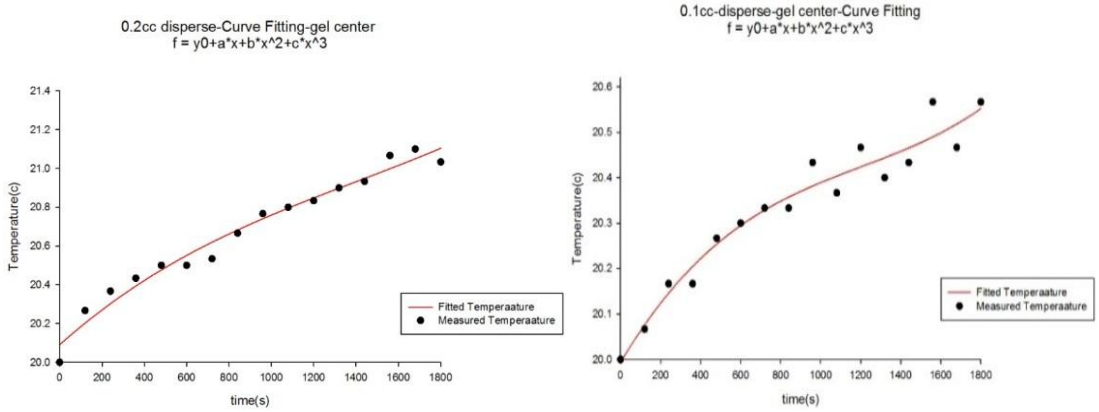

Figure 12. Left, 0.2*cc* ; right 0.1*cc* estimation function for central temperature for uniform injection.

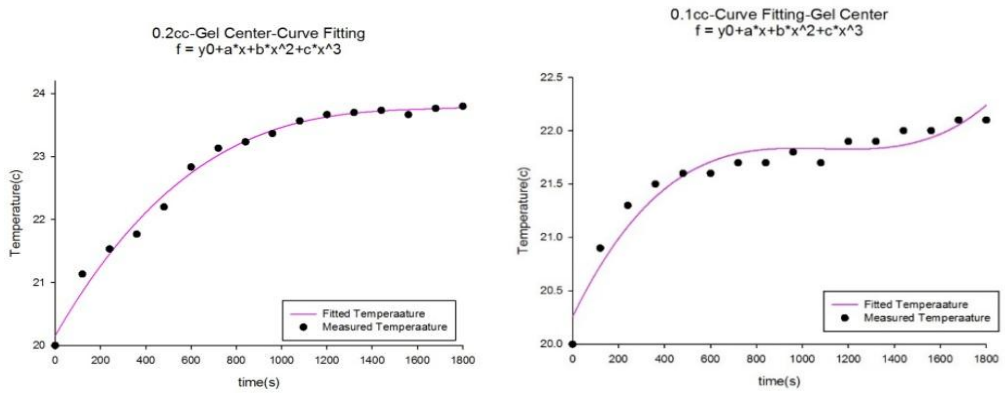

Figure 13. Left, 0.2*cc* ; right 0.1*cc* estimation function for central temperature for concentrated injection.

7. Special Absorption Rate (SAP)

SAR is the value of energy that the human tissue can absorb while subjecting to an external force. This force could be electrical fields electromagnetic or ultrasonic waves. In hyperthermia with the magnetic field, SAR is the heat value that the tissue (or gel) absorbs. It is needed to calculate the slope of the Temperature-Time curve to obtain SAR. According to the significance of the

p-value, we found out that a third-order polynomial is the best fit model for temperature curve estimation based on obtained experimental results. SAR can be calculated by Eq. 16 [14, 15].

$$SAR\,(\mathrm{w/\,m^3}) = \rho_{gel} C_{gel} \left.\frac{dT}{dt}\right|_{t=0} \tag{16}$$

where C_{gel} is tissue specific heat. In hyperthermia studies, SAR shows nano particles heat potential [16]. Figures 12 and 13, show the estimation of temperature curves for $0.2cc$ or $0.1cc$ injections for uniform and concentrated distributions in the central point of the experimental sample inside the magnetic coil. By using curve fitting tools and considering the significance of its p-value, we concluded that the best fit is a polynomial of degree three.

The third order estimation function has the following general form.

$$T_{Exp}(\mathrm{t}) = \mathrm{d}_0 + at + bt^2 + ct^3 \tag{17}$$

by derivation:

$$\left.\frac{dT_{Exp}(\mathrm{t})}{dt}\right|_{t=0} = a \tag{18}$$

The values for the parameters in Eq. 17 are depicted in Table 3.

Table 3. Constant values for estimation functions (uniform and concentrated distributions)

Samples\Parameters	d_0	a	b	c
Uniform Distribution (0.2 cc)	20.09	.001	-3.98e-7	9.5e-11
Uniform Distribution (0.1 cc)	19.99	.0007	-4.7e-7	1.33e-10
Concentrated Distribution (0.2 cc)	20.16	.0062	-3.66e-3	7.28e-10
Concentrated Distribution (0.1 cc)	20.26	.0044	-4.11e-6	1.25e-9

According to the definition for the SAR, we can compute its value by Eq. 19. The value for the SAR is summarized in Table 4. This table shows that the maximum value for the SAR corresponds to the concentrated distribution with 0.2cc injection of the magnetic fluid. Therefore, we can conclude that concentrated distribution significantly does a better job than the uniform distribution in the center of the sample. In addition, we can see that the value for SAR changes by changing the amount of the magnetic fluid injected into the tissue in both cases (uniform and concentrated distribution). This variation is too much; for example, it is almost 30 percent in this experiment.

$$SAR = 3900 \times 1011 \times a \tag{19}$$

Table 4. SAR for four samples

Samples	SAR
Uniform Distribution (0.2 cc)	3900
Uniform Distribution (0.1 cc)	2730
Concentrated Distribution (0.2 cc)	24200
Concentrated Distribution (0.1 cc)	17100

8. Conclusion

Researchers have studied hyperthermia with magnetic fluid as a cancer treatment method for a long time. In this work, some experiments are done on the agarose gel as an environment that is close to the tumor tissue. The magnetic field was simulated, and this field was calculated for some samples experimentally using a setup built for this purpose. Although there was no significant difference for the magnetic field in various sections of the samples inside the coil, the precise value of the magnetic field was obtained for the experiments. We perform a finite element method to calculate the temperature distribution in a

magnetic field using COMSOL software. Then, we compared the results for the simulation and the experimental ones for the samples with two types of distributions (uniform and concentrated) and two different concentrations of magnetic nanofluid injected into the tissue (in this case, agarose gel). The results showed that the temperature increases in concentrated distribution more than in uniform distribution. Additionally, the amount of injected nanofluid directly affects temperature increment. Specific absorption rate (SAR) is calculated via estimation of temperature function by experimental result. SAR has greater values in the concentrated distribution, and SAR increases by adding more injected nanofluid. In addition, as future work by our group, the effect of frequency, nanoparticle size and density, voltage, and heat source on the temperature distribution and finding the optimum values will be evaluated.

Acknowledgements

The authors want to thank Dr. Mohammad Haghpanahi, Dr. Mohammad Mehdi Attar, and Dr. Mehrdad Javidi for their help and support during this work.

Conflict of Interest Statement

The authors declare no conflict of interest.

References

[1] R. W. Habash, R. Bansal, D. Krewski, "Thermal therapy, part 2: hyperthermia techniques," *Crit Rev Biomed Eng.*vol. 34, no. 6, 2006.

[2] H. Richter et al., "Dynamic modeling, parameter estimation and control of a leg prosthesis test robot," vol. 39, no. 2, pp. 559-573, 2015.

[3] P. K. Gupta et al., "Numerical simulation for heat transfer in tissues during thermal therapy," *J Therm Biol.* vol. 35, no. 6, pp. 295-301, 2010.

[4] T. Byers *et al.* , "The American Cancer Society challenge goals: How far can cancer rates decline in the US by the year 2015? ," vol. 86, no. 4, pp. 715-727, 1999.

[5] K. Yue, C. Yu et al., "Numerical simulation of effect of vessel bifurcation on heat transfer in the magnetic fluid hyperthermia," Appl Therm Eng., vol. 69, no. 1-2, pp. 11-18, 2014.

[6] E.-H. Lee, C.-Y. Kim, Y.-H. J. C. A. P. Choa, "Magnetite nanoparticles dispersed within nanoporous aerogels for hyperthermia application," *Curr Appl Phys,* vol. 12, pp. S47-S52, 2012.

[7] H. Rahn, S. Schenk et al., "Tissue model for the study of heat transition during magnetic heating treatment," *IEEE Trans Magn*, vol. 49, no. 1, pp. 244-249, 2012.

[8] H. H. Pennes, "Analysis of tissue and arterial blood temperatures in the resting human forearm," *J Appl Physiol.,* vol. 85, no. 1, pp. 5-34, 1998.

[9] P. Yuan, "Numerical analysis of temperature and thermal dose response of biological tissues to thermal non-equilibrium during hyperthermia therapy," *Med Eng Phys.,* vol. 30, no. 2, pp. 135-143, 2008.

[10] A. F. Emery et al., "The use of heat transfer principles in designing optimal diathermy and cancer treatment modalities," *Int J Heat Mass Transf.,* vol. 25, no. 6, pp. 823-834, 1982.

[11] M. Javidi *et al.* , "Evaluation of the effects of injection velocity and different gel concentrations on nanoparticles in hyperthermia therapy," *J Biomed Phys Eng.,* vol. 4, no. 4, p. 151, 2014.

[12] A. R. Hajrasouliha, J. Springman, E. Parker, A. Washington, R. Akbari, A. Izadian, "Magnetic Nanoparticles Localization in Ophthalmologic Surgery," in *proc. 2019 IEEE International Conference on Electro Information Technology (EIT)*, 2019, pp. 505-508: IEEE.

[13] M. Mohammadzadeh, M. Shariatmadari, N. Riahi, and A. Komaee, "Feedback Decoupling of Magnetically Coupled Actuators," in *proc. 2021 IEEE/ASME International Conference on Advanced Intelligent Mechatronics (AIM)*, 2021, pp. 320-325: IEEE.

[14] E. Parker *et al.*, "Modeling of external self-excitation and force generation on magnetic nanoparticles inside vitreous cavity," *Mathematical Biosciences and Engineering*, vol. 18, no. 6, pp. 9381-9393, 2021.

[15] R. Akbari, Izadian, "Modeling and Control of Flywheel-Integrated Generators in Split-Shaft Wind Turbines," *Journal of Solar Energy Engineering*, vol. 144, no. 1, 2022.

[16] T. Samaras, A. Christ, "Effects of geometry discretization aspects on the numerical solution of the bioheat transfer equation with the FDTD technique," *Phys Med Biol.*, vol. 51, no. 11, p. N221, 2006.

[17] E. Rahmanian et al., "Numerical simulation of blood flow in centrifugal heart pump by utilizing meshless smoothed particles hydrodynamic method," *International Journal of Bio-Science and Bio-Technology*, vol. 7, no. 3, pp. 73-82, 2015.

[18] M. R. Rossi, "Experimental verification of numerical simulations of cryosurgery with application to computerized planning," *Phys Med Biol.*, vol. 52, no. 15, p. 4553, 2007.

[19] M. Adinehvand, C. Y. Lai, R. Hoseinnezhad, "Barrier-Lyapunov-Function-Based Backstepping Adaptive Hybrid Force/Position Control for Manipulator with Force and Position Constraints," in proc. *2021 American Control Conference (ACC)*, 2021, pp. 2266-2271: IEEE.

[20] Z.-S. Deng, "Mathematical modeling of temperature mapping over skin surface and its implementation in thermal disease diagnostics," *Comput Biol Med.*, vol. 34, no. 6, pp. 495-521, 2004.

[21] A. A. Golneshan, "Effect of heated region on temperature distribution within tissue during magnetic fluid hyperthermia using lattice Boltzmann method," *J Mech Med Biol.*,vol. 11, no. 02, pp. 457-469, 2011.

[22] M. Lahonian, "Numerical study of temperature distribution in a spherical tissue in magnetic fluid hyperthermia using lattice Boltzmann method," *IEEE Trans NanoBioscience.*, vol. 10, no. 4, pp. 262-268, 2011.

[23] A. E. Deatsch, "Heating efficiency in magnetic nanoparticle hyperthermia," *J Magn Magn Mater.*, vol. 354, pp. 163-172, 2014.

[24] M. Salloum et al., "Controlling nanoparticle delivery in magnetic nanoparticle hyperthermia for cancer treatment: experimental study in agarose gel," *Int J Hyperthermia.*, vol. 24, no. 4, pp. 337-345, 2008.